

Photocarrier recombination in $\text{Al}_y\text{In}_{1-y}\text{As}/\text{Al}_x\text{Ga}_{1-x}\text{As}$ self-assembled quantum dots

S. Raymond,* S. Fafard, and S. Charbonneau

Institute for Microstructural Sciences, National Research Council, Ottawa, Ontario, Canada K1A 0R6

R. Leon,[†] D. Leonard, P. M. Petroff, and J. L. Merz[‡]

Center for Quantized Electronic Structures (QUEST) and Materials Department and Electrical and Computer Engineering Department, University of California, Santa Barbara, California 93106

(Received 8 June 1995)

Ensembles of self-assembled quantum dots (QD's) are investigated using photoluminescence (PL) and resonant time-resolved PL in the visible spectrum. Faster carrier relaxation/recombination dynamics (~ 250 ps) are observed for resonant excitations. The influence of the temperature and the intensity of excitation is also measured by monitoring sharp spectral features (~ 200 μeV) obtained when probing the PL of small ensembles (~ 600 QD's). Temperature-independent linewidths are observed up to 70 K ($k_B T \gg 200$ μeV). For higher excitation intensity, however, the collective background, emitted by the ensemble of QD's, is enhanced relative to the amplitude of the individual sharp spectral features.

Recently, the spontaneous island formation in the Stranski-Krastanow growth mode of highly strained semiconductors has been exploited to produce self-assembled $\text{Al}_y\text{In}_{1-y}\text{As}/\text{Al}_x\text{Ga}_{1-x}\text{As}$ quantum dots (QD's) with emission in the visible (red) spectrum.¹⁻³ Nonresonant photoluminescence (PL) experiments, performed on ensembles with a different number of QD's, exposed the sharpness of the single-dot emission forming the smooth Gaussian line shape which is often observed when probing a larger number of slightly different QD's. On the other hand, resonant PL experiments revealed enhanced radiative recombinations for excitation energies permitting resonant phonon (multiphonon) relaxation,⁴ suggesting different zero-dimensional (0D) induced carrier/exciton relaxation mechanisms. Nonresonant time-resolved PL (TRPL) studies obtained with other self-assembled QD's confirmed a different carrier dynamics and/or temperature behavior.⁵ However, the influence of the temperature and of the intensity of excitation remains to be investigated in the case where sharp QD lines can be observed. Also, TRPL pumped resonantly in the excited states would help clarify the mechanisms pertinent to the photocarrier relaxation in small QD's, such as the restricted phonon-scattering rates⁶⁻⁸ or the Auger-like processes.⁹ Therefore, to further elucidate the effects of the 0D confinement on the carriers/excitons and the related dynamics, we present in this paper the results of resonantly excited TRPL, and the temperature and intensity behaviors of the sharp spectral features associated to the individual QD emission.

The sample used for this work was grown by molecular-beam epitaxy using the spontaneous island formation in the Stranski-Krastanow growth mode.¹⁰ From substrate to top, the layers grown are a GaAs (100) buffer, a 200-nm $\text{Al}_{0.35}\text{Ga}_{0.65}\text{As}$ barrier layer, the $\text{In}_{0.55}\text{Al}_{0.45}\text{As}$ QD layer, a 30-nm $\text{Al}_{0.35}\text{Ga}_{0.65}\text{As}$ barrier layer, and a thin GaAs cap layer. The QD layer is composed of a 2.1-nm quantum well, called the wetting layer

(WL), on top of which the QD's are formed. The QD's thus produced have a diameter of 18 ± 2 nm, a thickness of 3.2 nm, and their areal density is $200 \mu\text{m}^{-2}$. More detailed sample and growth descriptions have been published elsewhere.^{1,3} In this paper, we report on two QD ensembles obtained from the above sample, hereafter named ensembles *A* and *B*. Ensemble *A* was obtained by focusing the laser spot to a diameter of $\sim 80 \mu\text{m}$ on the as-grown sample, thus yielding a population of $\sim 10^6$ QD's. Ensemble *B* was achieved by defining a $3\text{-}\mu\text{m}^2$ mesa, resulting in a small group of ~ 600 QD's.² We first present the TRPL measurements obtained on ensemble *A*, and then discuss the temperature and intensity dependence of the emission spectra obtained with ensemble *B*.

For TRPL experiments, the optical excitation was provided by a frequency-doubled mode-locked Nd^{3+} : YAG laser synchronously pumping a dye layer, producing 5-ps pulses with a repetition rate of 4 MHz. The PL is then dispersed by a 0.75-m double spectrometer and detected by a 25-mm-diam cooled imaging photomultiplier tube (IPMT). Combined with a position computer, the IPMT gives the location of given photon events, allowing electronic gating of the signal and precise detection-energy selection.

Figure 1 shows the typical PL results obtained with ensemble *A*. The dashed curve of Fig. 1(a) displays the steady-state PL spectrum obtained when exciting non-resonantly above the barrier material, where relaxation in the QD's requires the emission of several phonons and may involve many processes. The spectral shape of the QD PL (at 1.887 eV) is a smooth Gaussian with a full width at half maximum (FWHM) of 46 meV.² The shoulder observed at 1.96 eV is attributed to PL from the WL. The solid curve of Fig. 1(a) is obtained when the sample is excited resonantly on the high-energy side of the Gaussian at 1.927 eV. Peaks appear at fixed energies below the excitation line, corresponding to phonon modes in the QD and barrier materials. For example, the dominant peaks labeled LO_1 and LO_2 appear, respective-

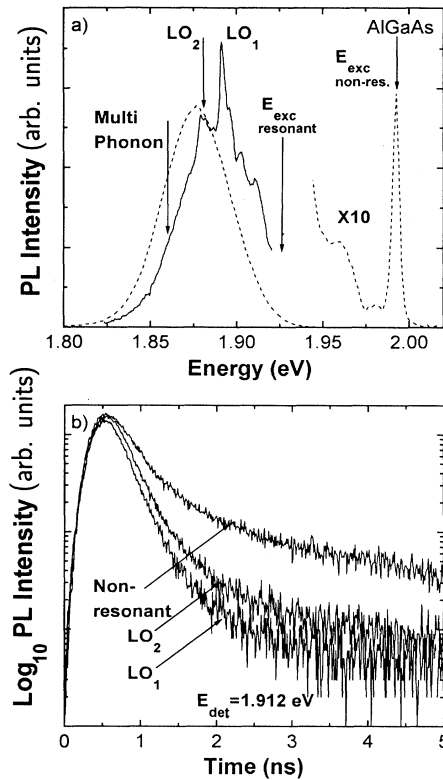


FIG. 1. Low-temperature PL of $\sim 10^6$ $\text{Al}_y\text{In}_{1-y}\text{As}/\text{Al}_x\text{Ga}_{1-x}\text{As}$ QD's. The dotted curve in (a) is obtained using an excitation energy (E_{exc}) above the barrier material, and the solid line is obtained for resonant excitation. The peaks LO_1 (LO_2) are observed at 35 meV (48 meV) below the excitation energy. In (b), the corresponding time-resolved spectra are obtained for $E_{\text{det}} = 1.912$ eV. The decay traces "Nonresonant," LO_1 and LO_2 , are thus obtained for $E_{\text{exc}} = 1.993$ eV, $E_{\text{exc}} = E_{\text{det}} + 35$ meV, and $E_{\text{exc}} = E_{\text{det}} + 48$ meV.

ly, 35 and 48 meV below the laser energy, and are associated to one GaAs-like and one AlAs-like phonon in $\text{Al}_x\text{Ga}_{1-x}\text{As}$.⁴ Similar phonon signatures have been observed in resonant TRPL spectra obtained with corrugated superlattices and were attributed to Raman or coherent Raman scattering.¹¹ Here, however, the phonon signatures are observed for a longer time scale and a wider spectral width than the exciting laser pulse. The observed decay times of the signal emitted a phonon away from the excitation (200–300 ps) are within our experimental resolution (~ 100 ps), whereas the Raman-scattering phenomena would appear to be instantaneous relative to the time scale involved here. This, therefore, confirmed the identification of the peaks observed in resonant excitation as being PL originating from QD's excited with an excess of phonon energy.

The decay characteristics of the PL signal excited in the various conditions illustrated in Fig. 1(a) have been investigated and are compared in Fig. 1(b). The three decay curves are obtained at different excitation wavelengths, but with the same detection energies (E_{det}), and thus probing equivalent QD's under various excitation

conditions. The curve labeled "nonresonant" was obtained when exciting above the barrier material, whereas the curves labeled LO_1 and LO_2 are obtained when exciting at $E_{\text{det}} + 35$ meV and at $E_{\text{det}} + 48$ meV, respectively. Clearly, the decay times for the QD PL are faster in cases of resonant excitation. Previous carrier relaxation studies performed with structures of higher dimensionalities have also demonstrated that faster cooling times can be obtained in the case of LO phonon-assisted relaxations, and that cooling rates are slower as the dimensionality is reduced.^{12–15} Here, for the excitation intensity of 1.4 $\text{nW}/\mu\text{m}^2$, the maximum number of pairs of photocarriers which can be generated among the 10^6 QD's probed is estimated to be $\sim 10^6$ per pulse for the nonresonant excitation, and much less for the other two curves. For the nonresonant case, most carriers are created in the barrier layers, and will subsequently relax to the 0D QD ground state. Some of the decay mechanisms available are carrier-carrier scattering, Auger-like processes, and (multi)phonon emission. The very low excitation intensity used reduces the possibility of carrier-carrier scattering and Auger-like processes. Relaxation by phonon emission can occur in several different ways: First, by direct trapping in the QD ground state by multiphonon emission. Second, the carriers can fall in a WL state, possibly with a nonzero wave vector, by phonon emission. After relaxation to the WL ground state, the carriers would relax to the QD ground state. If such a process occurs, the capture time between the WL and the QD ground state must be very fast since very little WL PL is observed. Every phenomenon discussed above involves different time constants, which might account for the nonsingle exponential decay curves observed in Fig. 1(b).

Figure 2 gives a summary of the various rise times and decay times observed for different detection energies. The rise time is defined here as the time necessary for the TRPL signal to reach its maximum value. Decay times have been obtained by fitting our results to a triple-exponential decay and keeping the dominant (fastest) component. Figure 2(a) shows the rise time for resonant (open symbol) and nonresonant (solid symbol) conditions. One observes that when detecting resonantly, one phonon energy below the excitation line, all rise times are faster. This effect is readily understood since resonant phonon-assisted capture is expected to be faster, independent of the precise nature of the capture process. The latter may include resonant absorption in excited states followed by resonant-phononic decay to the ground state, direct absorption in the ground state with simultaneous single-phonon emission, or multiple-phonon emission. Figure 2(b) shows the decay time for resonant (solid symbol) and nonresonant (open symbol) conditions. The nonresonant curve shows faster decay times with higher detection energy. This might be explained by an increased carrier confinement for higher emission energies. For example, QD's with diameters 1 or 2 nm smaller than the average diameter of 18 nm would have a reduced lifetime because the additional lateral confinement will increase the overlap of the wave functions, and have higher emission energies because the strongly quantized height is typically re-

lated to diameter by a constant aspect ratio. A similar trend is observed under resonant excitation conditions, with decay times that are shorter, consistent with the fact that a slow feed-in process will show up in the PL trace as a slow tail in the decay.^{5,16} The results suggest that exciting resonantly one LO phonon energy above the ground state of the QD's probed helps to bypass the slow relaxation processes that might take place in the non-resonant case, therefore speeding the decay of the TRPL signal. It is also interesting to compare recombination times for the cases where the relaxation process will require more than one phonon to the case of resonant excitation with an excess energy of exactly one phonon. For example, the "multiphonon" results in Fig. 2 are obtained by detecting ~ 65 meV below the excitation as illustrated in Fig. 1(a). For such excitations, in addition to one LO phonon, other smaller energy phonons will participate to lead to the ground-state radiative recombination. The measured recombination times for such multiphonon excitations, using excess energies close to but not equal to the LO-resonant excitation, are still much faster than the nonresonant above-barrier recombination times, suggesting efficient multiphonon carrier cooling.

PL measurements were performed on ensemble *B*. The sample was excited with a continuous-wave Ti:sapphire laser at 1.96 eV, and the resolution of the PL system is 80 μeV . Previous experiments² have shown that for a small number of QD's probed (~ 600), sharp spectral features

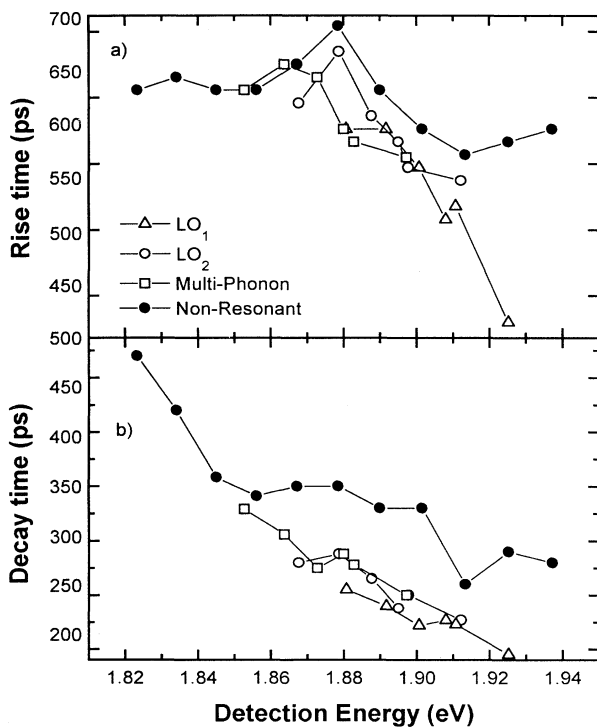


FIG. 2. Rise times as defined in the text (a) and decay times (b) as a function of detection energy. Solid (open) symbols show the results obtained for nonresonant (resonant) excitation conditions. The instrumental response of the system is 420 ps for the rise time and 100 ps for the decay time.

start appearing on top of the smooth Gaussian spectrum. This suggested that the overall PL spectrum results from the convolution of a number of very sharp intrinsic emission lines, each corresponding to the emission line of individual QD's. Figure 3 shows the QD PL spectrum obtained for ensemble *B* at different temperatures with an excitation power of 250 $\text{nW}/\mu\text{m}^2$. The spectra exhibit several sharp spectral features of similar magnitude with a FWHM ranging from 190 to 400 μeV . Other mesas excited above the barrier material ($E_{\text{exc}} = 2.0$ eV) with very low power densities (25 $\text{nW}/\mu\text{m}^2$) have shown some spectral features of ~ 100 μeV . Each sharp feature corresponds to the PL trace of a few QD's, typically one to six,¹ emitting at similar wavelengths. The nonzero PL signal observed in between adjacent lines is due to the finite intrinsic emission linewidth of each single QD. This collective background has to be distinguished from the dark count signal, since the former is a property of the QD population and the latter is a property of the set-up.

The spectra shown in Fig. 3 have been shifted to align the sharp lines at all temperatures. Spectral features for which the intensity level remains well above the collective emission background show very little broadening as the temperature is increased up to 70 K. Some lines, such as

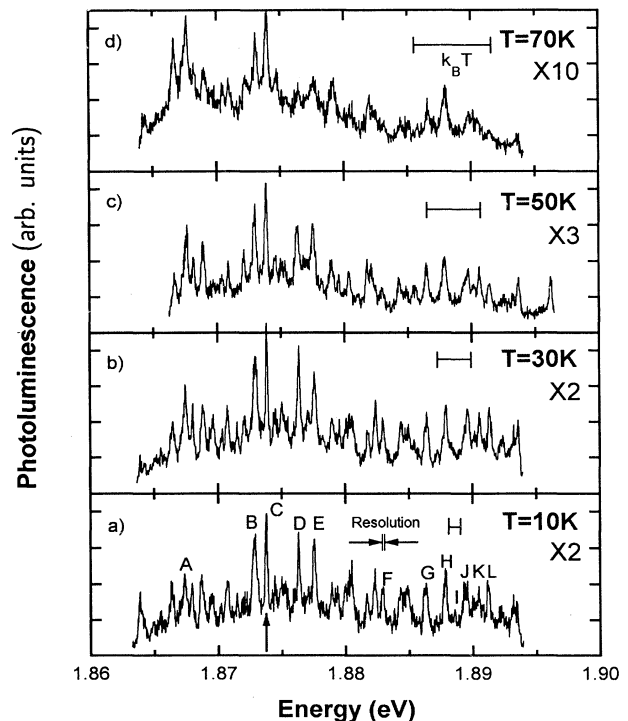


FIG. 3. PL spectrum for ensemble *B* (~ 600 $\text{Al}_y\text{In}_{1-y}\text{As}/\text{Al}_x\text{Ga}_{1-x}\text{As}$ QD's) at different temperatures obtained with an excitation intensity of 250 $\text{nW}/\mu\text{m}^2$. The energy scale is for the 10-K spectrum. At higher temperatures the spectra were shifted to align the peak indicated by an arrow. We also show the resolution of our setup and the evolution of the thermal energy for comparison.

G , do show some broadening, although much less than the increase in the thermal energy ($k_B T$). This small effect can be attributed to the background noise in the experiment, since at 70 K the PL intensity has decreased by a factor of 10 due mostly to thermionic emission,^{5,17} and several lines are barely seen above the dark count level for such small excitation intensities. These temperature-independent linewidths are in contrast with the case of a quantum well where the 2D density of state permits a continuum of energy leading to thermal broadening of the emission line. The difference between the two cases lies in the density of states, and the behavior in temperature observed here clearly is the one expected for a δ -function-like density of states with no significant carrier population in the radiative excited state(s).

Figure 4 shows the evolution of the PL as a function of excitation power at low temperatures. The low-intensity spectrum ($150 \text{ nW}/\mu\text{m}^2$) shows the same features as in Fig. 3(a). As the intensity is increased, most of the sharp spectral features (A to F) observed lose amplitude with respect to the collective background, and in some cases even disappear completely, the most striking example being peak H . Lines that remain identifiable tend to stay narrow, although some of them do show evidence of broadening (peak B , for example). In some cases, higher intensities have little effect (J , K , and L) or even cause the emergence of new features. Line I , for example, is barely detected at low intensity, but progressively rises above the background as the intensity is increased. These observations cannot be related to temperature effects, since Fig. 3 demonstrates that increasing the temperature does not change the spectrum significantly. An increase in the photocarrier populations is more likely to be at the origin of the new spectral features. Neglecting the dynamics in the higher-energy states, the steady-state population in the QD ground state is given by the product of the photogenerated carrier flux, $\Phi(I_{\text{ex}})$, and the lifetime in the QD ground state, τ_{GS} . Here, for $\tau_{\text{GS}}=300 \text{ ps}$ and for the intensities of $150 \text{ nW}/\mu\text{m}^2$, $1.5 \mu\text{W}/\mu\text{m}^2$, and $4.5 \mu\text{W}/\mu\text{m}^2$, $\Phi(I_{\text{ex}})\tau_{\text{GS}}$ is, respectively, 0.002, 0.02, and 0.06 per QD.¹⁸ The presence of carriers in the QD at the moment of recombination is expected to have an effect on the emission energy.^{19,20} For example, for higher populations, charged excitons or biexcitons would emit at energies different than the QD exciton energies. The corresponding changes in the emission energies are expected to be between a fraction of meV to a few meV, depending on the exact nature of the interaction and the resulting binding energies. The fact that several QD's are simultaneously probed complicates the observation of such fine excitonic structures or splittings, but the emission can be redistributed at different energies, which could be seen as a rise of the collective emission background, or in some cases the new QD emission lines can cause the emergence of new spectral features such as line I . Alternatively, some of the observed spectral modifications could also be explained, in part, if at the lowest intensities only some of the QD's emit, and the remaining QD's start to contribute only at higher excitations. Radiative recombination from excited states would also give lines at higher ener-

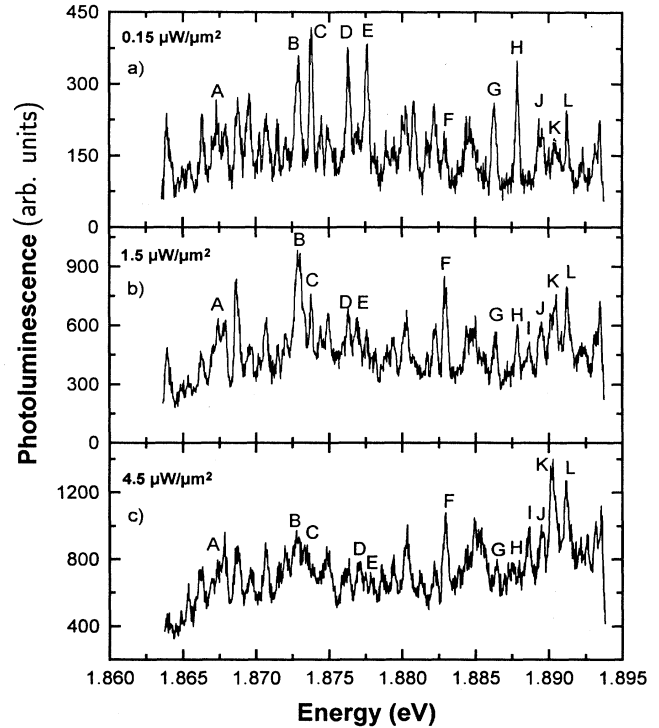


FIG. 4. PL spectrum at 4 K of ensemble B ($\sim 600 \text{ Al}_x\text{In}_{1-y}\text{As}/\text{Al}_x\text{Ga}_{1-x}\text{As}$ QD's) for different excitation intensities. The excitation energy was 1.960 eV.

gies, but this is an unlikely scenario here, given that the large interlevel spacing associated to these small QD's would lead to peaks several tens of meV on the high-energy side of the ground-state emission.⁴ Further studies with fewer QD's, or with structures where electrons or holes can be electrically injected independently, would help to clarify the origins of the rich variety of phenomena observed here as a function of the exciting intensity.

In summary, we performed resonant time-resolved spectroscopy on a self-assembled QD sample. Lifetimes of the order of 200 to 400 ps were obtained. It was shown that the carrier dynamics is enhanced for resonant QD excitation, permitting single or multiple phonon relaxation of the excess energy. The temperature and intensity dependence of the PL spectra for a small ensemble of QD's was also investigated. The sharp spectral features obtained in the PL spectra do not broaden as the temperature is increased up to 70 K, clearly demonstrating the 0D nature of the density of states. Finally, at low temperatures it was shown that for higher excitation intensity, the collective background emitted by the ensemble of QD's is enhanced relative to the amplitude of the individual sharp spectral features.

This research was supported by NSF Science and Technology Center QUEST (DMR No. 91-20007), by AFOSR Grant No. F49620-92-J-0124. One of us (S.R.) would also like to acknowledge NSERC for their additional support.

- *Also at Department of Physics, University of Ottawa, Ottawa, Ontario, Canada K1N 6N5.
- †Present address: Department of Electronic Materials Engineering, The Australian National University, Canberra, ACT, 0200, Australia.
- ‡Present address: Department of Electrical Engineering, University of Notre Dame, Notre Dame, IN 46556-5602.
- ¹R. Leon, P. M. Petroff, D. Leonard, and S. Fafard, *Science* **267**, 1966 (1995).
- ²S. Fafard, R. Leon, D. Leonard, J. L. Merz, and P. M. Petroff, *Phys. Rev. B* **50**, 8086 (1994).
- ³R. Leon, S. Fafard, D. Leonard, J. L. Merz, and P. M. Petroff, *Appl. Phys. Lett.* **67**, 521 (1995).
- ⁴S. Fafard, R. Leon, D. Leonard, J. L. Merz, and P. M. Petroff, *Phys. Rev. B* **52**, 5752 (1995).
- ⁵G. Wang, S. Fafard, D. Leonard, J. E. Bowers, J. L. Merz, and P. M. Petroff, *Appl. Phys. Lett.* **64**, 2815 (1994).
- ⁶P. D. Wang, C. M. Sotomayor Torres, H. McLelland, S. Thomas, M. Holland, and C. R. Stanley, *Surf. Sci.* **305**, 585 (1994).
- ⁷U. Bockelmann, *Phys. Rev. B* **48**, 17 637 (1993).
- ⁸H. Benisty, C. M. Sotomayor Torres, and C. Weisbuch, *Phys. Rev. B* **44**, 10 945 (1991).
- ⁹A. L. Efros, V. A. Kharchenko, and M. Rosen, *Solid State Commun.* **93**, 281 (1995).
- ¹⁰D. Leonard, K. Pond, and P. M. Petroff, *Phys. Rev. B* **50**, 11 687 (1994).
- ¹¹D. S. Jiang, X. Q. Zhou, M. Oestreich, W. W. Rühle, R. Nötzel, and K. Ploog, *Phys. Rev. B* **49**, 10 786 (1994).
- ¹²Y. Rosenwaks, M. C. Hanna, D. H. Levi, D. M. Szymd, R. K. Ahrenkiel, and A. J. Nozik, *Phys. Rev. B* **48**, 14 675 (1993).
- ¹³R. Ferreira and G. Bastard, *Phys. Rev. B* **40**, 1074 (1989).
- ¹⁴D. Morris, D. Houde, B. Deveaud, and A. Regreny, *Superlattices Microstruct.* **15**, 309 (1994).
- ¹⁵A. C. Maciel, C. Kiener, L. Rota, J. F. Ryan, U. Marti, D. Martin, F. Morier-Gemoud, and F. K. Reinhart, *Appl. Phys. Lett.* **66**, 3039 (1995).
- ¹⁶C. Van Hoof, Ph.D. thesis, Katholieke Universiteit Leuven, 1992.
- ¹⁷Modeling the QD PL emitted at an energy E and temperature T , considering the Gaussian distribution of the ground-state energies centered at E_0 with a broadening Γ , and the thermionic emission out into the barrier material with band-gap energy E_b , we obtain $PL(E, T) \propto \exp\{-[(E - E_0)/\Gamma]^2\} / [1 + \rho \exp\{-(E_b - E)/k_B T\}]$, where $\rho \approx 2 \times 10^8$.
- ¹⁸A 30% reflection at the sample surface and a 0.5% absorption in the wetting layer were included in the calculation of $\Phi(I_{ex})$.
- ¹⁹A. Wojs and P. Hawrylak, *Phys. Rev. B* **51**, 10 880 (1995).
- ²⁰D. S. Citrin, *Phys. Rev. Lett.* **69**, 3393 (1992).